

Spin Freezing in the Geometrically Frustrated Pyrochlore Antiferromagnet $Tb_2Mo_2O_7$

B. D. Gaulin,⁽¹⁾ J. N. Reimers,^{(2),(a)} T. E. Mason,^{(1),(b)} J. E. Greedan,⁽²⁾ and Z. Tun⁽³⁾

⁽¹⁾*Department of Physics and Astronomy, Institute for Materials Research, McMaster University, Hamilton, Ontario, Canada L8S 4M1*

⁽²⁾*Department of Chemistry, Institute for Materials Research, McMaster University, Hamilton, Ontario, Canada L8S 4M1*

⁽³⁾*AECL Research, Chalk River Laboratories, Chalk River, Ontario, Canada K0J 1J0*

(Received 12 June 1992)

The magnetic metal ions in the cubic pyrochlore $Tb_2Mo_2O_7$ form an infinite three-dimensional network of corner-sharing tetrahedra with a very high potential for frustration in the presence of antiferromagnetism. We have performed neutron scattering measurements which show short-range spatial correlations that develop continuously with decreasing temperature, while the characteristic time scale for the fluctuating moments decreases dramatically below $T_f \sim 25$ K. Therefore, this *pure* material, which possesses frustration *that is purely geometrical in origin*, displays a spin-glass state at low temperatures.

PACS numbers: 75.25.+z, 75.40.Gb, 75.50.Ee, 75.50.Lk

Materials containing antiferromagnetically coupled magnetic moments on geometrical units that frustrate the formation of a collinear ordered state often exhibit unusual behavior at low temperatures. The experimental realizations of these structures are made up of two types of locally frustrated building blocks: triangles and tetrahedra. In two dimensions such lattices can be formed by a network of edge-sharing triangles to make the familiar triangular lattice [1], or by a network of corner-sharing triangles to make the *kagomé* lattice [2]. In three dimensions edge-sharing tetrahedra give rise to the face-centered-cubic lattice, while a network of corner-sharing tetrahedra [3] form structures found in spinel, Laves, and pyrochlore crystals.

The frustration inherent in the combination of antiferromagnetic interactions and a network of tetrahedra can be appreciated by considering four antiferromagnetically coupled spins on a single tetrahedron. For simplicity we discuss the Ising case, although frustration occurs for vector spins as well. As shown in Fig. 1(a), arranging any two spins into an up-down pair does not allow the other spins to align up or down without frustrating two of the six interactions. The ground state for such a lattice therefore has a greater spin degeneracy (which depends on the number of degrees of freedom of the individual spins) than in a comparable unfrustrated lattice.

Many pyrochlores have the chemical formula $A_2B_2O_7$ and most of them crystallize in the cubic space group $Fd\bar{3}m$. Both the *A* and *B* metal sublattices form an infinite three-dimensional network of corner-sharing tetrahedra, as shown in Fig. 1(b). Spin-glass-like behavior has been observed in the pyrochlore magnets $Y_2Mo_2O_7$ [4], $Y_2Mn_2O_7$ [5], and $Tb_2Mo_2O_7$ [4] as evidenced by susceptibility cusps, irreversibilities, and diffuse magnetic neutron scattering over an extended range of temperature. Neutron and x-ray diffraction measurements on all three compounds show no evidence of positional disorder. In particular, cation disorder can be ruled out on the basis of a bond-length argument; the rare-earth ion simply does not fit in the transition metal

site [6]. Nonstoichiometric oxygen content seems to be the most likely form of structural disorder. However, diffraction profile refinements indicate that any such nonstoichiometry must be below the 1% level. *These results strongly suggest that the spin-glass-like behavior is intrinsic to the pure pyrochlore magnets.*

We have carried out a detailed neutron scattering study of the static and dynamic behavior of $Tb_2Mo_2O_7$ in powder form. To our knowledge, single-crystal samples of sufficient size for neutron scattering have not yet been produced. We chose to study $Tb_2Mo_2O_7$ due to the very large moment present at the Tb^{3+} site ($\sim 9\mu_B$). Both of the metal ions are magnetic but the Tb^{3+} moment is approximately 9 times larger than that at the Mo^{4+} site. The neutron scattering experiment measures dynamical spin correlation functions of the form $\langle S_i(0)S_j(t) \rangle$, where $\langle \dots \rangle$ represents a thermal average. Therefore the contribution to the neutron scattering signal from Tb^{3+} - Tb^{3+} correlations is almost 2 orders of magnitude stronger than that from Mo^{4+} - Mo^{4+} correlations and an order of magnitude stronger than that from Tb^{3+} - Mo^{4+} correlations. The experiment is thus sensitive primarily

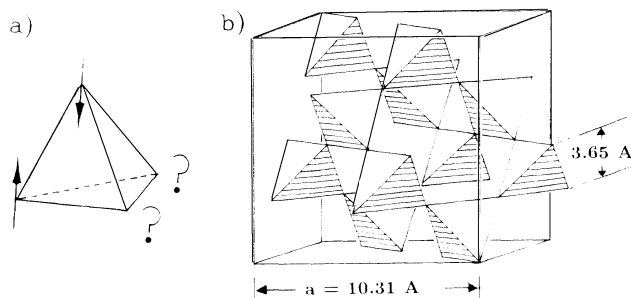


FIG. 1. (a) The frustration inherent between four antiferromagnetically coupled spins on a single tetrahedron is illustrated. (b) The three-dimensional network of corner-sharing tetrahedra formed by one of the metal atom sublattices in the pyrochlores. An outline of the cubic unit cell (with room-temperature lattice dimensions displayed for $Tb_2Mo_2O_7$) is also shown.

to Tb^{3+} - Tb^{3+} correlations and it is reasonable to think of the magnetism associated with the Mo^{4+} sites as contributing an additional interaction path for the Tb^{3+} moments. This large moment of Tb^{3+} allowed us to study the inelastic magnetic spectrum from a powder sample with relatively high-energy resolution. Since the spin-glass-like behavior seen in the bulk properties of the pyrochlores with a single magnetic site ($\text{Y}_2\text{Mn}_2\text{O}_7$ and $\text{Y}_2\text{Mo}_2\text{O}_7$) is similar in that seen in $\text{Tb}_2\text{Mo}_2\text{O}_7$, we expect the results reported in this Letter to be generally applicable to this entire class of frustrated magnets.

Measurements were performed on the N5 triple axis neutron spectrometer of the NRU reactor at Chalk River Laboratories. Scans were made with the spectrometer in two different configurations. Low and high frequency resolution scans were performed using a constant scattered neutron frequency of $E_f/h = 3.52$ and 1.10 THz, respectively. The low frequency resolution mode was achieved using the (1,1,1) reflection of a Si monochromator and the (0,0,2) reflection of pyrolytic graphite (PG) to analyze the frequency of the scattered beam. The (1,1,1) reflection of Si has a systematic absence for $\lambda/2$ neutrons. Also, a PG filter was placed in the scattered beam to reduce higher-order contamination. Collimation before and after the sample was 0.66° and 0.8° , respectively. This configuration resulted in a measured frequency resolution of ~ 0.28 THz. The high frequency resolution mode was achieved using the (0,0,2) reflection of PG as both monochromator and analyzer. A cooled beryllium filter was placed in the scattered beam to eliminate higher-order contamination. The incident and scattered beam collimation was 0.44° and 0.24° , respectively. This configuration resulted in a measured instrumental frequency width of ~ 0.045 THz. All measurements were made on the same sample of $\text{Tb}_2\text{Mo}_2\text{O}_7$ used in Ref. [4]. The powder sample was loaded in a vanadium sample can with a helium exchange gas to provide thermal contact. It was then mounted in a closed-cycle helium refrigerator. In the high-resolution mode, data were collected at ten temperatures between 11 and 50 K, with particular emphasis on the region near previously measured anomalies at $T_f \sim 25$ K.

Wave-vector scans made in the low frequency resolution mode with the analyzer set to accept zero frequency scattering are shown as a function of temperature in Fig. 2. Two sharp peaks, identified as the (111) and (113) nuclear Bragg peaks, could be observed near $Q \sim 1$ and 2 \AA^{-1} at all temperatures.

Strong diffuse scattering, reminiscent of a liquid structure factor, is seen to develop continuously below 50 K, with the growth of this scattering being most pronounced below 30 K. The measured intensity is seen to grow with decreasing temperature at all wave vectors studied. At low temperatures, strong diffuse peaks are seen near $Q = 1.0$ and 2.0 \AA^{-1} with a minimum between them at $\sim 1.5 \text{ \AA}^{-1}$. This diffuse scattering is qualitatively similar to the energy-integrated diffraction data previously re-

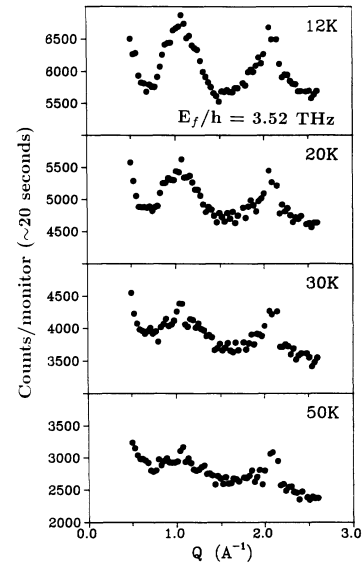


FIG. 2. Low-resolution (see text) elastic wave-vector scans are shown for four temperatures in $\text{Tb}_2\text{Mo}_2\text{O}_7$. Strong diffuse scattering peaks, with approximately temperature-independent wave-vector widths, develop continuously below 50 K. The intensity at 50 K is due primarily to nuclear incoherent scattering from the vanadium sample cell, and to magnetic incoherent scattering from the sample itself.

ported [4]. Very interestingly, the width in Q space of the diffuse peaks is approximately temperature independent at the temperatures presented here even though the strength of the scattering increases with decreasing temperature. This indicates that while the static (relative to the inverse of the frequency resolution of the measurement) magnetic moment within a correlation volume is markedly increasing with decreasing temperature below 50 K, the spatial extent of the correlated regions is not changing with temperature. The wave vector of the diffuse peaks is consistent with a short-range ordering of the Tb^{3+} moments with a (111) wave vector. The half-width of the diffuse peak can be taken as a measure of the correlation length which we estimate at $5 \pm 1 \text{ \AA}$. A correlated droplet of Tb^{3+} spins therefore includes spins on nearest-neighbor tetrahedra only.

Constant- $|Q|$, high-resolution frequency scans were performed near the strongest diffuse peak at $Q = 1.0 \text{ \AA}^{-1}$, but carefully avoiding the (111) nuclear Bragg peak, and near a minimum of the profile at $Q = 1.5 \text{ \AA}^{-1}$. Representative frequency scans at $Q = 1.0 \text{ \AA}^{-1}$ are shown in Fig. 3. An empty sample cell scan has been subtracted from these data sets. The frequency distributions are dominated by a quasielastic peak which increases in intensity as the temperature is lowered. The measured line shape is well described by a detailed balance factor times a Lorentzian in frequency:

$$S(Q, \nu) = \frac{h\nu}{k_B T} \left[1 - \exp\left(\frac{-h\nu}{k_B T}\right) \right]^{-1} \frac{A}{\nu^2 + \nu_c^2}.$$

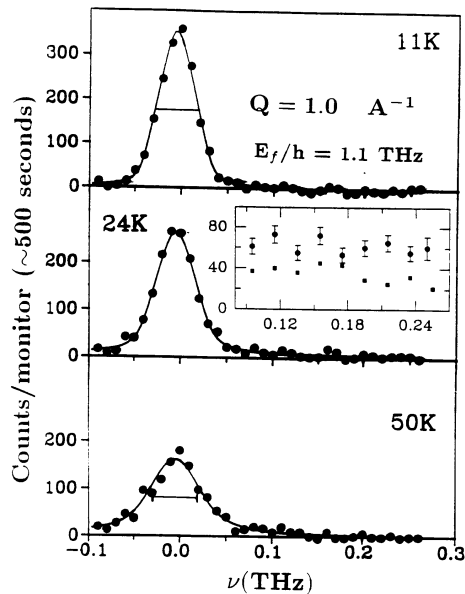


FIG. 3. High-resolution (see text), inelastic, constant $|Q|=1.0 \text{ \AA}^{-1}$ scans are shown for three temperatures in $\text{Tb}_2\text{Mo}_2\text{O}_7$. An empty sample cell data set has been subtracted from the signal. The solid lines are fits to the data described in the text. The horizontal lines in the top and bottom panels indicate the resolution width of the measurement. The inset in the middle panel shows raw data from identical scans taken in the wings of the scattering some 15 h apart at 24 K, demonstrating extremely slow dynamics near T_f .

This expression was then convoluted with the frequency resolution function corresponding to the appropriate spectrometer configuration and fit to the data. Fits to $S(Q, \nu)$ of this form are shown as the solid lines in Fig. 3. The values for the peak intensity at $\nu=0$ and for ν_C , the characteristic frequency describing the width of the distribution, extracted from this fitting procedure are shown in Figs. 4(a) and 4(b). These values are not particularly sensitive to the range of ν included in the fit.

As can be seen from Fig. 4(a), the diffuse peak intensity approximately doubles between 50 and 11 K, but evolves as a smooth function of temperature. Over the entire range of temperature investigated, its behavior is well described by $S(Q, \nu=0) \sim -\ln(T/T_0)$, where $T_0 \sim 200 \text{ K}$. There is no anomaly present in the $S(Q, \nu=0, T)$ data near $T_f \sim 25 \text{ K}$, although the behavior in the immediate vicinity of T_f will be discussed separately. At the minimum of the Q -dependent scattering, $Q=1.5 \text{ \AA}^{-1}$, the frequency width of the distribution is only weakly temperature dependent, if at all. This is as expected for scattering dominated by nuclear incoherent processes, and these ν_C values are indicative of the minimum frequency width which this experiment can discern. Below $\sim 25 \text{ K}$, the magnetic scattering at $Q=1.0 \text{ \AA}^{-1}$ is characterized by roughly the same ν_C values as that at $Q=1.5 \text{ \AA}^{-1}$, indicating the frequency width of the scattering has dropped below the resolution limit.

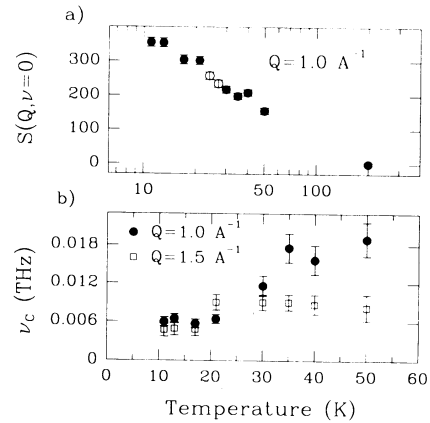


FIG. 4. (a) Fit values for $S(Q=1.0 \text{ \AA}^{-1}, \nu=0)$ are shown as a function of temperature. The data at 24 and 27 K show signs of nonequilibrium behavior and are labeled separately from the other temperature data points. (b) The fit values of ν_C are shown as a function of temperature at the maximum and minimum of the magnetic scattering, $Q=1.0$ and 1.5 \AA^{-1} , respectively. As the frequency width of the $Q=1.5 \text{ \AA}^{-1}$ data is resolution limited, these data show the spins to be fluctuating on the time scale of $[\nu_C(T \leq 20 \text{ K})]^{-1}$ above $T_f \sim 25 \text{ K}$, and static below.

However, above $T_f \sim 25 \text{ K}$, ν_C at $Q=1.0 \text{ \AA}^{-1}$ rises well above that at $Q=1.5 \text{ \AA}^{-1}$, demonstrating that the moments at these temperatures are fluctuating on a time scale comparable to that of the measurement. This effect is seen qualitatively by comparing the resolution limit full width at half maximum with the data well above and below T_f , and is shown in Fig. 3 for the 11 and 50 K data at $Q=1.0 \text{ \AA}^{-1}$.

It should be noted that frequency-dependent contamination of the incident beam with higher-order (λ/n) neutrons [7] makes the absolute values extracted for ν_C somewhat inaccurate. However, this correction is only weakly frequency dependent over the range of energies probed and is temperature independent.

The inelastic data, shown in Fig. 3, taken at $\nu > 0.1 \text{ THz}$ are the result of two scans taken $\sim 15 \text{ h}$ apart and then added together to improve counting statistics. At all temperatures *except* 24 and 27 K these scans were identical. However, we found that in the vicinity of T_f the data *did not* reproduce, with systematically higher scattering measured in the later of the two scans performed after changing the temperature from either 21 to 24 K, or 24 to 27 K. This is shown in the inset to the middle panel of Fig. 3 for the 24 K data, in which the early and late time data are displayed as squares and circles, respectively. Similar behavior is seen at 27 K. Consequently we see that the cooperative behavior near T_f is such that extremely slow spin dynamics are relevant and true equilibrium behavior is never observed during the course of the measurement. This is at least qualitatively similar to the extreme critical slowing down observed [8] in the random-field Ising system $\text{Fe}_{0.46}\text{Zn}_{0.54}\text{F}_2$ near its

transition temperature. Scans around $\nu=0$ were not repeated. Values for $S(Q=1.0 \text{ \AA}^{-1}, \nu=0)$ at 24 and 27 K are included in Fig. 4(a) as open circles, and it can be seen that they follow the same continuous behavior described above. One should bear in mind, however, that these values may also display very slow time dependence.

These measurements strongly suggest that the spin-glass-like anomaly observed in the dc susceptibility at ~ 25 K is a dynamical phase transition. At this transition the short-range ordered spins transform from being dynamic roughly on the time scale of $\sim [\nu_C(T \leq 20 \text{ K}) \sim 0.005 \text{ THz}]^{-1} = 2 \times 10^{-10}$ sec to being static on that time scale. Since the anomalies which are seen in the bulk properties occur at the same temperature and at much lower frequencies, including the dc response [4], the slowing down of the characteristic time scale for the spin fluctuations must be very dramatic near this temperature.

The ground-state properties of geometrically frustrated magnets is a longstanding problem in theoretical physics of considerable current interest. Anderson was the first to consider the problem of antiferromagnetically coupled spins on a lattice of corner-sharing tetrahedra [3]. He argued that no long-range ordered state should exist for classical Ising spins at low temperature. Recent mean-field theory [9] and Monte Carlo simulations [10] support this conclusion. A similar picture emerged from Villain's work on classical Heisenberg spins on this lattice and he coined the term "cooperative paramagnet" [11] to describe the low-temperature state of such a system. These conclusions have also received support from Monte Carlo simulation techniques [12]. Initial work [13] regarding quantum Heisenberg spins on a lattice of corner-sharing tetrahedra suggests unconventional, long-range dimer ordering with a sublattice structure.

Experimentally, spin-glass-like behavior has recently been observed in the weakly disordered, stacked *kagomé* lattice compound $\text{SrCr}_{8-x}\text{Ga}_{4+x}\text{O}_{19}$ (SCGO) [14], where diffuse neutron scattering has been observed from powder samples down to 1.5 K. The frequency width of the inelastic spectrum in SCGO extends out past 2 THz (~ 90 K) even at the lowest temperature examined. Further, a total moment sum rule analysis yielded a ratio of the mean-square fluctuating moment to frozen moment at low temperatures in excess of 4. The low-temperature state described by these measurements is therefore strongly fluctuating.

The picture that emerges from our measurements contrasts with that described above for SCGO. The Tb^{3+} spins on the corner-sharing tetrahedral lattice in $\text{Tb}_2\text{Mo}_2\text{O}_7$ order locally into short-range ordered droplets at relatively high temperatures (compared to T_f). The characteristic size of these short-range ordered regions does not increase with decreasing temperature. However, the characteristic time scale of the fluctuating moments slows down as the temperature is lowered, with a dramatic spin freezing occurring below $T_f \sim 25$ K. At low tem-

peratures, all of the magnetic scattering appears to be elastic.

The behavior of this pure, geometrically frustrated magnet is reminiscent of that seen in chemically disordered spin glasses such as CuMn [15] and amorphous MnSi [16] in which neutron scattering identification of the occurrence of a phase transition is highly dependent on the frequency resolution of the experiment.

We benefited from helpful discussions with G. Aeppli, D. P. Belanger, A. J. Berlinsky, C. Kallin, and Y. J. Uemura. This work was supported in part by the Natural Sciences and Engineering Research Council of Canada and by the Ontario Centre for Materials Research. Two of us (B.D.G. and T.E.M.) gratefully acknowledge the hospitality of Chalk River Laboratories. One of us (B.D.G.) acknowledges the support of the Alfred P. Sloan Foundation.

-
- (a) Present address: Department of Physics, Simon Fraser University, Burnaby, British Columbia, Canada V5A 1S6.
- (b) Present address: Department of Solid State Physics, Risø National Laboratory, 4000 Roskilde, Denmark.
- [1] G. H. Wannier, *Phys. Rev.* **79**, 357 (1950).
- [2] I. Syozi, in *Phase Transitions and Critical Phenomena*, edited by C. Domb and M. S. Green (Academic, New York, 1972), p. 269.
- [3] P. W. Anderson, *Phys. Rev.* **102**, 1008 (1956).
- [4] J. E. Greedan, J. N. Reimers, C. V. Stager, and S. L. Penny, *Phys. Rev. B* **43**, 5682 (1991), and references therein.
- [5] J. N. Reimers, J. E. Greedan, R. K. Kremer, E. Gmelin, and M. A. Subramanian, *Phys. Rev. B* **43**, 3387 (1991), and references therein.
- [6] J. N. Reimers and J. E. Greedan, *J. Solid State Chem.* **72**, 390 (1988).
- [7] See R. A. Cowley, G. Shirane, R. J. Birgeneau, and H. J. Guggenheim, *Phys. Rev. B* **15**, 4292 (1977), in which this effect was treated by a scale factor, varying by $\sim 30\%$, applied to the measured intensity as $\Delta\nu/\nu$ changed from 0 to ~ 0.5 for $\nu=3.52$ THz.
- [8] D. P. Belanger, V. Jaccarino, A. R. King, and R. M. Nicklow, *Phys. Rev. Lett.* **59**, 930 (1987).
- [9] J. N. Reimers, A. J. Berlinsky, and A.-C. Shi, *Phys. Rev. B* **43**, 865 (1991).
- [10] R. Liebmann, in *Statistical Mechanics of Periodic Frustrated Ising Systems* (Springer, Berlin, 1986), p. 117.
- [11] J. Villain, *Z. Phys. B* **33**, 31 (1978).
- [12] J. N. Reimers, *Phys. Rev. B* **45**, 7287 (1992).
- [13] A. B. Harris, A. J. Berlinsky, and C. Bruder, *J. Appl. Phys.* **69**, 5200 (1991).
- [14] C. Broholm, G. Aeppli, G. P. Espinosa, and A. S. Cooper, *Phys. Rev. Lett.* **65**, 3173 (1990); A. P. Ramirez, G. P. Espinosa, and A. S. Cooper, *Phys. Rev. Lett.* **64**, 2070 (1990).
- [15] A. P. Murani and A. Heidemann, *Phys. Rev. Lett.* **41**, 1402 (1978); Y. J. Uemura, S. M. Shapiro, and L. E. Wenger, *J. Appl. Phys.* **57**, 3401 (1985).
- [16] G. Aeppli, J. J. Hauser, G. Shirane, and Y. J. Uemura, *Phys. Rev. Lett.* **54**, 843 (1985).